IEEE Access
Multidisciplinary | Rapid Review | Open Access Journal

Received 15 August 2025, accepted 9 September 2025,
date of publication 16 September 2025, date of current version 22 September 2025.

Digital Object Identifier 10.1109/ACCESS.2025.3610524

RESEARCH ARTICLE

Energy Management Solution for Islanding Based on a Dynamic Neuro-Fuzzy-Optical Microscope Algorithm

AHMED OSAMA[1], DALIA ALLAM[1], AHMED F. ZOBAA[2], (Senior Member, IEEE), AND MAGDY B. ETEIBA[1]

[1]Electrical Engineering Department, Faculty of Engineering, Fayoum University, Faiyum 63514, Egypt
[2]Design and Physical Sciences, Brunel University of London, UB8 3PH Uxbridge, U.K.

Corresponding author: Ahmed F. Zobaa (azobaa@ieee.org)

ABSTRACT Ensuring continuity of service is a primary objective in power systems. In grid-connected microgrids (MGs), islanding poses a significant threat to this continuity. Conventional approaches mitigate islanding by disconnecting the MG immediately after separation from the main grid to prevent overload and ensure safety, but this results in service interruption. This study proposes a dynamic islanding management strategy that maintains uninterrupted service using an optimal dynamic neuro-fuzzy–optical microscope algorithm (OMA). The method integrates a convolutional neural network (CNN), fuzzy logic (FL), and the novel OMA optimizer in a two-stage framework. In the first stage, the CNN detects islanding based on active current and voltage measurements at the point of common coupling (PCC) and their dominant harmonic components, obtained from a hybrid MG model. This model is comprising solar panels, wind turbines, a biomass generator, and a storage system. Signal and image processing techniques prepare the measurements for CNN implementation. Upon islanding detection, the second stage is activated, where FL predicts the penalty factor and OMA optimally manages economic power sharing between the grid and the MG. This integration enables safe load coverage without damaging MG components. Performance benchmarking against Quadratic Interpolation Optimization (QIO) and Hunger Games Optimizer (HGO) demonstrates that OMA achieves higher accuracy, faster convergence, and lower execution time. Validation across five scenarios under normal, islanding, and risky operating conditions confirms the method's effectiveness, reliability, and economic benefits, achieving a 223.7% revenue improvement over the baseline with the shortest execution time. The proposed approach offers a robust and intelligent solution to the islanding problem, ensuring continuous and cost-effective microgrid operation.

INDEX TERMS Islanding, energy management, fuzzy logic, CNN, optical microscope algorithm.

NOMENCLATURE

Acronyms

η_{Bio}	biomass generator efficiency.
η_{ch}	charging efficiency.
η_{dis}	discharging efficiency.
γ_{tem}	the temperature factor.
D_{sol}	the derating factor.
FC_M	marginal fuel consumption.
FC_{NL}	no-load fuel consumption.
GR_{inc}	incident radiation.
GR_{STC}	incident radiation in STC.
LHV_{gas}	Lower heating values of gas.
LHV_{wood}	Lower heating values of wood.
P_{Bat}	the energy stored in the battery bank.
$P_{Bio}(t)$	biomass power.
$P_{sol,R}$	the solar panel's rated power.
$P_{W,R}$	the wind turbine's rated power.
P_W	the wind power.

The associate editor coordinating the review of this manuscript and approving it for publication was Qiang Li.

RSS_{Bio}	biomass resources consumption.
$TEM_{c,STC}$	the cell temperature in STC.
TEM_c	the cell temperature.
WS	the wind speed.
WS_{in}	the cut-in speed.
WS_{off}	the cut-off speed.
WS_R	the rated wind speed.
CNN	convolution neural network.
FL	fuzzy logic.
OMA	optical microscope algorithm.
PCC	point of common coupling.

I. INTRODUCTION

Recently, there has been a new avenue in the power strategy relying on dilation in merging renewable energy resources with the main grid in the distribution system. Therefore, there is a persistent need to manage energy between the main grid and the other microgrids economically and dynamically. That's why, introducing and developing novel techniques is of high priority to enhance the power-sharing between the main grid and the MG efficiently and economically and to help in solving some serious problems associated with the grid-connected microgrids. One of the most important issues in the grid-connected microgrid is the islanding problem. Several studies have been carried out to detect the islanding and the only solution that has been offered for this problem is the disconnection of the microgrid upon detection of islanding to protect MG from damage even an account of service continuity to the load. Islanding may lead to safety hazards, damage of MG components, and a reduction of power quality for the customers due to asynchronous re-closure [1]. Therefore, detecting the islanding should be fast for making the optimal decision for the energy management plan [2].

In the realm of islanding detection strategies, the approaches presented in the literature can be classified into remote, communication-based, passive, and active techniques. The passive detection approach has been regarded as one of the most economical techniques relying on the measured signals at the point of common coupling (PCC) such as voltage, current, and frequency. It has different techniques such as measuring the rate of change of frequency w.r.t a predefined threshold by monitoring the q-axis current controller and comparing with the threshold value [3]. Another method has been proposed based on the mean of the absolute positive sequence voltages difference and when this value has exceeded a certain value over a specific period, the islanding has been detected with a very low non-detection zone (NDZ) [4]. A matrix pencil method has reconstructed the voltage signal to calculate the magnitudes of the phasors through the Discrete Fourier Transform where islanding has been indicated using the sign of the magnitude difference of the raw and the reconstructed signals [5]. The phase jump detection method has been introduced as a passive method but it has some challenges such as an undefined threshold value and false trapping caused by a capacitor bank or motor starting [6]. In [7], the islanding detection has been based on the phase angle of the positive sequence components of voltages that equals zero in normal operation while it is more than zero during abnormal conditions. The unbalanced voltage can also identify the islanding by monitoring the change of the reactive power where the exceeded reactive power will lead to over-voltage and low reactive power means an under-voltage condition. This variation was compared with the threshold value to disconnect the microgrid upon the occurrence of islanding [8]. Islanding detection was provided by smart technique by residual neural networks, wavelet transform and Stockwell transform as, wavelet transform and Stockwell transform provided the feature images of islanding and non-islanding conditions which it entered to the residual neural networks to detect the islanding condition using deep learning-based residual neural networks in conjunction with hybrid signal processing techniques [9]. Harmonic distortion is one of the main approaches that can detect the islanding mode by comparing the total harmonic distortion with a predefined threshold value [10]. The dominant harmonic components such as the second harmonics of the voltage and the current signals have been used as inputs to a machine learning algorithm for islanding detection as in [1]. The second main type of islanding detection method is the active methods which have lower NDZ which leads to better accuracy than the passive approaches but they are of higher costs where their operation is based on the injection of a small periodic signal of voltage or frequency of the grid [1]. One of the active approaches is the Sandia voltage shift where the power of the inverter drops with the voltage during the islanding providing positive feedback to the controller to trap the relay when this drop exceeds the threshold value [11].In [12], the voltage signals were injected and the current signals were measured at PCC to estimate the impedance then the relay was trapped if the variation of impedance exceeded the limits. Remote detection communication-based methods based on external communication between the microgrid and the main grid can provide more reliability for the system but it is of high cost. The microgrid elements operate in the same geographical locations so the phase shift among the voltage phases can be measured accurately via phasor measurement units as in [13], The data has been fed to the control unit and protection devices to determine the state of operation. Another technique that depends on a centralized controller to monitor the stats of the circuit breakers is called the transfer trip approach. This approach has the superiority of monitoring each element individually when a radial connection is used [14]. In the islanding detection schemes, convolutional neural networks (CNNs) were utilized to perform detection and classification based on image recognition. Time-series data were transformed into two-dimensional representations using the wavelet transform with a Morse wavelet, after which the resulting images were processed by the CNN to identify islanding conditions [15]. In the previous research on the

islanding problem, the main target is detecting the islanding mode, and the solution is the disconnection of the microgrid (MG)after the detection process. Consequently, part of the connected loads may lose the service upon the occurrence of islanding. Proposing an innovative strategy to minimize the impacts of the islanding mode and the load shedding should be investigated. Managing the energy among the islanded microgrid devices may be considered the lighted avenue to address the islanding impacts. To the authors' best knowledge, implementing energy management as an innovative solution to guarantee the continuity of services for minimizing load shedding during the islanding has not been investigated in the literature.

In the context of energy management systems, there are various methods of managing energy between the main grid and the microgrids. They can be divided into traditional methods, schedule methods, and online methods. The role of the storage system in enhancing energy management and power charging is essential, and it provides flexibility to the system to make optimal decisions. Storage systems can be classified based on their power and energy density characteristics, and combined into a hybrid configuration to leverage the advantages of each category [16]. Consequently, integrating the storage system with the power system is recommended to improve the power system's stability and reliability, provide flexible solutions for energy management challenges, enhance power system performance with renewable resources, and manage the modes (vehicle-to-grid, grid-to-vehicle) of electric vehicles connected to the grid [16]. In traditional methods, actions are taken according to the availability of energy without considering the real-time price. Fuzzy logic, neural network, PI controller, or if-else statements can be used for this approach [17], [18], [19]. While the management over a certain time horizon using the predicted input data had low uncertain levels is schedule method [20]. The decision has considered the real-time price for the optimal solution as the minimum operating cost and improving the grid reliability. In [21], a multi-objective algorithm has been used to decrease the operating cost, loss of power supply, and emissions while increasing the renewable factor. The energy of the storage system has been managed as a scheduling plan. An electric spring was employed in a standalone DC microgrid as a storage system to enhance flexibility and effectiveness in the demand-side management approach. A distributed adaptive droop control strategy was introduced, improving power sharing among the different energy resources [22]. Another technique has been presented to minimize the cost by using an extended particle swarm optimization algorithm (PSO) and adaptive dynamic programming [23]. During the online method, the state of the microgrid was investigated step by step over the time horizon, and the decisions were taken for every time step individually to be suitable for real-time operation where the state of charge of the battery system (SOC) and the real-time price are the main inputs for the dynamic methodology. A real-time optimization function was introduced for online management without a dynamic factor to control and constrain the SOC [24]. Hossain et al. [25] have modified the fitness function by adding a penalty factor for controlling SOC and obtaining the optimum solution of the problem by using a modified PSO.

Previous research focuses on energy management during normal operation or the detection of the islanding mode and disconnecting the MG without managing the energy and storage system. To fill in the research gaps, this paper presents a smart neuro-fuzzy-OMA optimizer solution for the islanding problem that is proposed for the first time, depending on the consolidation of convolution neural networks (CNN) based smart detection of islanding with fuzzy logic (FL)-based optimal online power management technique. This contribution offers a complete solution to islanding that ensures the continuity of service to the load instantly and dynamically as soon as the islanding problem is detected. In the proposed methodology, a hybrid grid-connected microgrid model consisting of solar panels, wind turbines, battery banks, and biomass-generating units has been designed. The proposed methodology is implemented through a main program with a modular structure comprising four interconnected modules. The first module is a simulated model, executed within the program to generate measurements under various operating scenarios. The second module is a CNN responsible for detecting islanding events and identifying potentially risky situations. The third module is the FL system designed to provide a penalty factor that adapts to changes in operating conditions, thereby guiding the optimizer toward improved energy management performance. The final module is the optimization unit, which performs the online energy management process. These four modules are fully integrated and executed within the main program, forming an interactive framework that delivers a dynamic and cost-effective solution to the islanding problem. The constructed model provides the voltage and current states at PCC as well as the signal processing and the image processing techniques. CNN provides a smart detection of islanding based on the voltage and current signals measured at PCC and the dominant harmonics components caused by islanding obtained by the Fourier transform of the measured signals. FL has been working in conjunction with the optimization technique to provide an optimal dynamic decision that assures the optimal continuity of service to the load during islanding. The optimal operation of the microgrid generating units as well as the storage system has been accomplished under normal and islanding conditions. To prove the validity and superiority of the proposed technique, five scenarios at normal and islanding operating conditions during various time steps have been tested. Furthermore, the baseline case has been investigated and the results have been tabulated for more verification of the proposed methodology. To enhance the reliability of the proposed scheme, a novel optimization

algorithm (OMA) has been selected for implementation in this complex problem, aiming to provide greater accuracy and efficiency. For more verification of the optimization process, three distinct optimization algorithms have been implemented and their results have been compared together to ensure the leading performance of the selected algorithm in achieving the optimal solution with a minimum operating cost and ensuring the reliability of the microgrid and continuity of service to the load during the islanding in addition to protecting the microgrid components from damage. The main contribution can be listed as follows:

- A novel integration of CNN, fuzzy logic FL, and OMA to address the islanding problem in microgrids.
- It introduces a dynamic, non-interruptive solution for the islanding problem, enhancing operational reliability without disconnecting the microgrid from the main grid upon detection of islanding.
- The approach dynamically manages power sharing between the grid and the microgrid, optimizing economic efficiency and energy distribution.
- The methodology is validated through various scenarios, demonstrating its effectiveness under both normal and islanding conditions.
- Three different optimization algorithms, highlighting the superior performance of the proposed OMA in achieving the lowest operational costs and maintaining service continuity.

In this work, CNN is used for smart detection of islanding, and the scheme uses fuzzy logic incorporated with an optimization algorithm to decrease the cost and improve the microgrid's reliability. The parts of this article are structured as follows. Section II identifies the modeling of the MG elements. The fitness function and the constraints are explained in section III and section IV respectively. Section V provides the proposed algorithm, FL, and CNN operation. The simulation, numerical implementation, results, and comparisons are discussed in section VI. Finally, section VII is the conclusion.

II. SYSTEM DESCRIPTION AND MODELING

The microgrid is connected to the main grid to exchange energy and improve reliability. The microgrid has three wind turbines with 10 Kw rated power and four solar panels with 5 Kw. It is provided with a battery bank with a capacity of 30 kWh. In addition, a 20 Kw biomass generator is added to the microgrid to cooperate with the battery bank to obtain minimum operating cost and improve reliability, especially during islanding conditions. The system's configuration and the operation's methodology can be shown in Figure 1. The hierarchical structure can be shown in Figure 2 to clear the steps of the methodology. The sizing of the microgrid components is obtained by using HOMER. The parameters of each component can be presented as the cut-in, cut-off, and rated speed equal to 3, 25, and 10 Km/h for wind turbines respectively. The derating factor is 0.88 and the efficiency equals 0.204 for solar panels. The efficiency of the converter is 0.95. The biomass parameters are defined as gasification efficiency equal to 0.7 and biomass fuel cost is 0.1 \$/Kg. The slope of fuel is 0.2998 (kg/h/kW). The lower heating value equals 5.5 MJ/kg, Density equals 0.72 kg/m^3. However, the battery bank parameters are listed as a round-trip efficiency equal to 0.8 and maximum discharging and charging currents equal to 24.3 A and 16.7 A respectively. The capacity ratio is 0.403. While the maximum charge rate and rate constants are 1 A/Ah and 0.827 h^{-1} respectively. The system modeling can be presented for MG elements.

A. SOLAR POWER

It can be estimated as a function of temperature and radiation. The solar power (P_{sol}) can be estimated by the following equation [25], [26]:

$$P_{sol} = P_{sol,R} D_{sol} \frac{GR_{inc}}{GR_{STC}} \left(1 + \gamma_{tem} \left(TEM_c - TEM_{c,STC}\right)\right) \tag{1}$$

where the $P_{sol,R}$ gives the solar panel's rated power. The D_{sol} is the derating factor. Although GR_{inc} and GR_{STC} provide incident radiation at the calculated time step and standard test conditions (STC), respectively. The cell temperature is presented by TEM_c. However, $TEM_{c,STC}$ indicates the cell temperature in STC. The γ_{tem} expresses the temperature factor.

B. WIND POWER

It is determined mainly based on the wind speed [25], [27]. The following equation provides its calculation:

$$P_W = \begin{cases} P_{W,R} \times \left(\dfrac{WS^3 - WS_{in}^3}{WS_R^3 - WS_{in}^3}\right) & WS_{in} \le WS \le WS_R \\ P_{W,R} & WS_R \le WS \le WS_{off} \\ 0 & otherwise \end{cases} \tag{2}$$

where the $P_{W,R}$ presents the wind turbine's rated power. However, the WS and the WS_R indicate the wind speed and the rated wind speed respectively. The cut-in and the cut-off speed are expressed as WS_{in} and WS_{off} respectively.

C. BATTERY MODEL

A battery bank is used as a storage system. It provides flexibility and improves the reliability of the MG to achieve optimal operating cost by exchanging energy with the main grid through charging / discharge cycles [28]. It is modeled as the two-tank dynamic model system [29]. This model estimates the maximum charging and discharging power for every time step which helps to find the optimal solution. The stored energy is calculated as [28]:

- Charging mode: The power is absorbed during this mode (P_{abs}) and the stored energy is updated using the

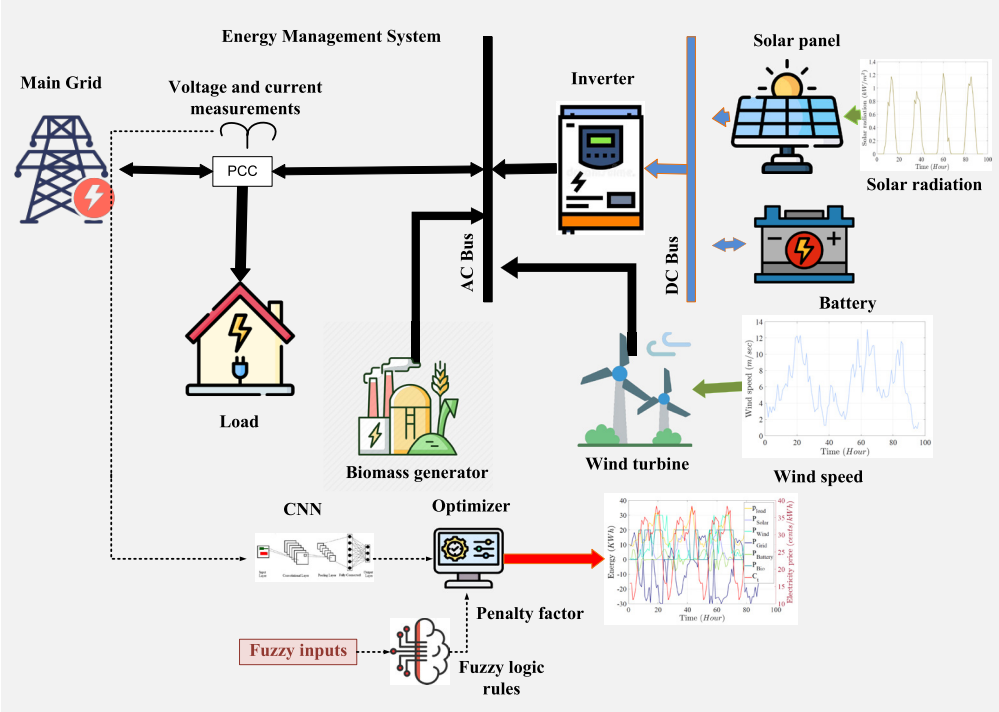

FIGURE 1. Scheme of the complete solution of a microgrid islanding problem.

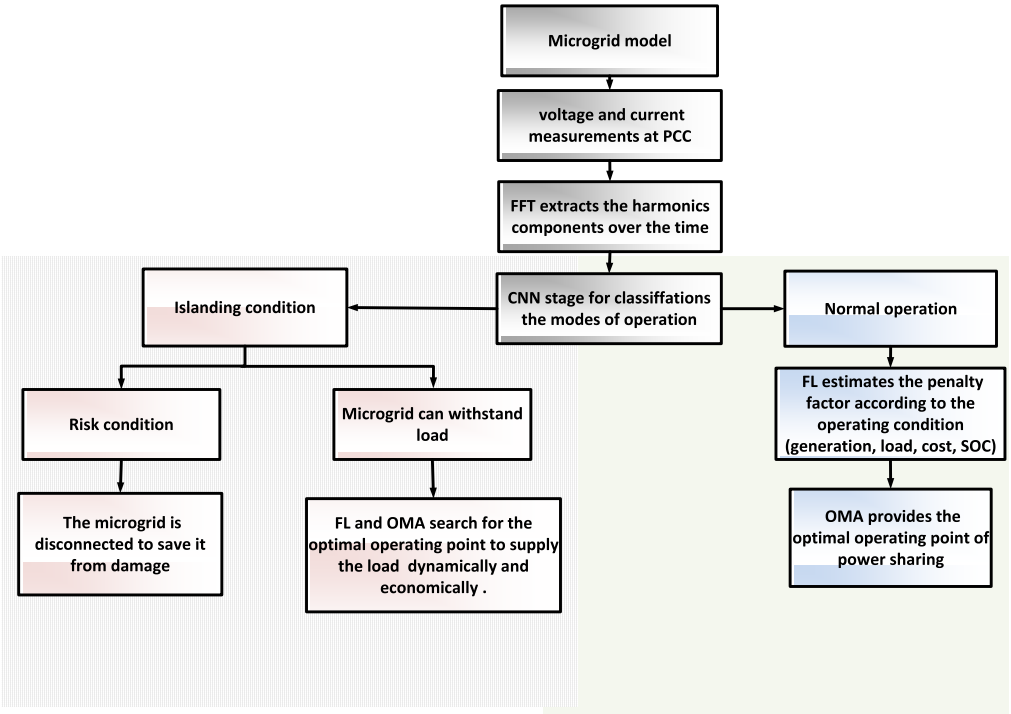

FIGURE 2. The hierarchical structure of the proposed approach.

following equation:

$$P_{Bat}(t) = P_{Bat}(t-1) + P_{abs}(t) \times \eta_{ch} \tag{3}$$

- Discharging mode: The power is dissipated (P_{dsp}) in this case and the energy stored becomes as:

$$P_{Bat}(t) = P_{Bat}(t-1) - \frac{P_{dsp}(t)}{\eta_{dis}} \tag{4}$$

where the η_{ch} and the η_{dis} are the efficiencies of the charging and discharging cycles respectively.

D. BIOMASS MODEL

The electrical energy is generated by the biochemical process in the residues of agricultural crops through the gasifier, which transforms the crops into gas [30], [31]. Thus, this fuel is fed to the generator to produce electricity. Fuel consumption is considered to be a linear function as a diesel generator. The power of the biomass generator can be obtained at each time step as [32]:

$$P_{Bio}(t) = \left(\frac{\eta_{bio} LHV_{gas} RSS_{Bio}(t)}{LHV_{wood}} - FC_{NL} P_{Bio,rated} \right) / FC_M \tag{5}$$

where $P_{Bio}(t)$ donates the biomass power. The RSS_{Bio} is the biomass resources consumption. The η_{Bio} gives the efficiency of the biomass generator. The LHV_{gas} and the LHV_{wood} express Lower heating values of gas and wood respectively. while the no-load and Marginal fuel consumption (kg/h/kW) are presented by FC_{NL} and FC_M respectively. Therefore, the fuel consumption is estimated as follows:

$$\begin{aligned} &\text{fuel consumption(t)} \\ &= \left(\frac{LHV_{gas}}{LHV_{wood}} \right) \times \left(FC_{NL} P_{Bio,rated} + FC_M P_{Bio}(t) \right) / \eta_{Bio} \end{aligned} \tag{6}$$

III. THE PROPOSED APPROACH

The proposed technique offers a complete solution for dynamic energy management to enhance reliability during islanding, save the microgrid from damage, and reduce the cost. The operating cost is calculated through exchanging energy with the main grid by the following equation [33], [34], [35]:

$$\text{operating cost} = \sum_{t=o}^{T} C_T(t) \times P_G(t) \tag{7}$$

where the P_G presents the power of the main grid with a (+) sign if the microgrid is buying energy while the (-) sign if the microgrid is selling energy. The C_T is the real-time price of the main grid (cents/kWh). However, the previous equation is suitable for the baseline method and offline techniques but needs updating for the method dynamically. The cost function is upgraded to force the system to charge the battery bank under a certain condition and save the SOC over time. A dynamic penalty factor is added to guide the scheme in making the optimal discussion [24], [36]. In this work, real-time pricing, the SOC, and renewable generation can cover the load or not. While the real operating cost and comparison between different techniques are determined from the equation in 7. The proposed cost function uses a dynamic penalty factor which is calculated each time step by the fuzzy rules and it is formulated as follows:

$$\begin{aligned} \text{cost fitness}(t) = {} & C_T(t) \times P_G(t) + PenF\,(SOC_{max} - SOC(t)) \\ & + \text{biomass operating cost(t)} \end{aligned} \tag{8}$$

where $PenF$ presents the dynamic penalty factor. The optimizer individually operates every time step to simulate real-time operation. In addition, the fuzzy rules guide the optimizer through the dynamic penalty factor which improves the microgrid performance with human logic. The main steps of the methodology can be listed below:

1) Grid-connected microgrid model simulation on MATLAB and operated within the main software.
2) Measure V and I signals at PCC using the simulation model.
3) Signal processing stage of V, I signals.
4) Image processing stage of the signals.
5) CNN for islanding detection.
6) Online dynamic power management based on fuzzy basic and OMA optimizer to make smart economical decisions about the supply load of the microgrid using the available energy to meet the load considering the maximum required current needed by the load and drawn from the microgrid.

IV. THE CONSTRAINTS AND LIMITATIONS

The proposed method has several constraints which can be listed as:

1) The maximum energy limit that can be bought or sold with the main grid is 30 kW.
2) The power balance between the generating energy and absorbed should be achieved.

$$P_W + (t) P_{sol}(t) + P_G(t) + P_{Bio}(t) = P_B(t) + P_L(t) \tag{9}$$

where P_B is the battery's power that has a + sign for charging mode and a - sign for discharging mode. The load power is expressed by P_L.

3) The energy absorbed or dissipated shouldn't exceed the limits calculated by the dynamic two-tank model [29].
4) The power of the biomass generator should not exceed its rated power.
5) The SOC should vary between the maximum and the minimum limits.

$$SOC_{min} \leq SOC(t) \leq SOC_{max} \tag{10}$$

where the upper and lower limits of SOC are 100% and 10% respectively.

The performance indices are determined using different factors which are used to evaluate the system performance (FPI) and make the decision for service continuity. These factors can be listed as

1) Voltage variation from the reference value which has a maximum value 5 % [37].

$$\text{FPI}(1) = \left| V - V_{ref} \right| \tag{11}$$

2) Total harmonic distortion of voltage signals from the frequency spectrum of the waveform by FFT.

$$\text{FPI}(2) = \frac{\sqrt{\sum_{n=2}^{m} V_n^2}}{V_1} \tag{12}$$

3) Total harmonic distortion of current signals.

$$\text{FPI}(3) = \frac{\sqrt{\sum_{n=2}^{m} I_n^2}}{I_1} \tag{13}$$

4) Voltage-frequency factor, which presents the balance between the demand and the generated power, and introduces the accepted range of frequency deviation during operation [38].

V. THE PROPOSED ALGORITHM TECHNIQUE

An optical microscope optimizer is applied in cooperating with FL and the proposed technique detects the islanding condition by CNN. The following subsections explain the proposed algorithm.

A. OPTICAL MICROSCOPE ALGORITHM

The optimizer relies on the process of repetitive zoom-in and magnification of small objectives by a microscope [39]. This process finds the target from the level of the naked eye and reaches the lenses of a microscope [39]. The eyepiece has several sets of lenses to achieve the best magnification. Four main steps were introduced and listed as follows [39]:

1) Naked eye: it gets the information about the problem, neglecting its shape and size.
2) Objective lens: the initial target was observed and the image magnification factor, called magnifying power (MP), is estimated with fixed steps.
3) Eyepiece: the objective lens was further magnified and its MP then the microscope's total magnification was multiplied by the magnifying power of the objective lens and the eyepiece.
4) optimal target: comparison among each magnification cycle was established to get the optimal solution.

The target objective is magnified through two phases (objective lens, eyepiece). These two stages are only applied to the iteration process,g_j gives j^{th} potential population size target where j = 1,2,3,..., PS and the other population size is equal to PS. The optimal solution is offered at the end of the iteration process with the maximum number of iterations ($iter_{max}$). The principle of compound microscopes models the total magnification power and it is calculated as [39] and [40]:

$$MP_{tot} = MP_L \times MP_E \tag{14}$$

where MP_L and MP_E are the magnifying power of the objective lens and the eyepiece, respectively, Therefore, the magnifying power of the objective lens is determined from the range of helpful magnification that it has minimum and maximum magnification equal to 2.5x to 100x with a numerical aperture (NP) value of 0,08 to 1.40. The updated target can be obtained from the following equation:

$$Mg_{jnew} = Mg_j + 1.4 \times M^s \times Mg_{best} \tag{15}$$

where the Mg_{best} indicates the optimal target. However, M^s is the magnification scale, which is a random value from zero to one for initial magnification. The Mg_j gives the initial target. Therefore, the current target is compared to the modified one and then the Mg_{best} is selected from the better of both. The eyepiece magnifies the target further after the objective lens is used. The magnification space is needed to estimate the effect of the eyepiece based on the distance between the current target (j) and another target (i)from the population. This process determines the local search space and the compared target is chosen randomly. In addition, it provides an effective exploitation of the local search space [39], [40].

$$\text{Magnification space} = \begin{cases} Mg_i - Mg_j & f(Mg_j) \geq f(Mg_i) \\ Mg_j - Mg_i & f(Mg_j) < f(Mg_i) \end{cases} \tag{16}$$

where $f(Mg)$ presents the objective function. The useful range of target magnification through this stage starts from 10x magnification power with a numerical aperture equal to 0.35 and ends at 25x magnification power with a numerical aperture equal to 0.55. Therefore, the modifying target is determined by [39]:

$$Mg_{jnew} = Mg_j + 0.55 \times M^s \times \text{Magnification space} \tag{17}$$

As in the previous phase, the updated target is compared with the current target, and the better is presented as the optimal target objective Mg_{best}. The flow chart of the OMA can be shown in Fig.3.

B. FUZZY LOGIC

FL improves the performance of dynamic energy management problems. Consider the time of use price, SOC, and the generation of renewable generators. It provides a dynamic penalty factor to optimally control the charging and discharging cycles of the battery bank [41]. In addition to reducing operating costs and providing a suitable SOC, it improves system reliability [42]. The fuzzy rule can be identified as an IF-THEN statement that links the antecedent of the rule and the consequence of the rule [43]. After adjusting FL based on the data collected and experts in the domain, the desired result is obtained. FL is formed from fuzzifier, rules, inference and defuzzification of output [44]. The rules tie between inputs and output in the IF-THEN statement and are expressed as linguistic terms that are more elastic and applicable to real-time problems than crisp logic [45]. Therefore, FL is implemented with three inputs and one output through a Mamdani-based inference to minimize the operating cost and enhance the charge cycle of the battery bank. The fuzzy has been tuned empirically. The inputs are the real-time price, the net power results from the difference between renewable generation and the demand load (Pnet), and SOC as shown in figure 4. The inputs are entered into the fuzzification process to be applied for rules by the memberships, then the output from the inference is fed to defuzzify through the center of gravity. The output presents the penalty factor for the amount of energy and its direction for each microgrid element to guide the optimizer in estimating the solution of the online approach, where the

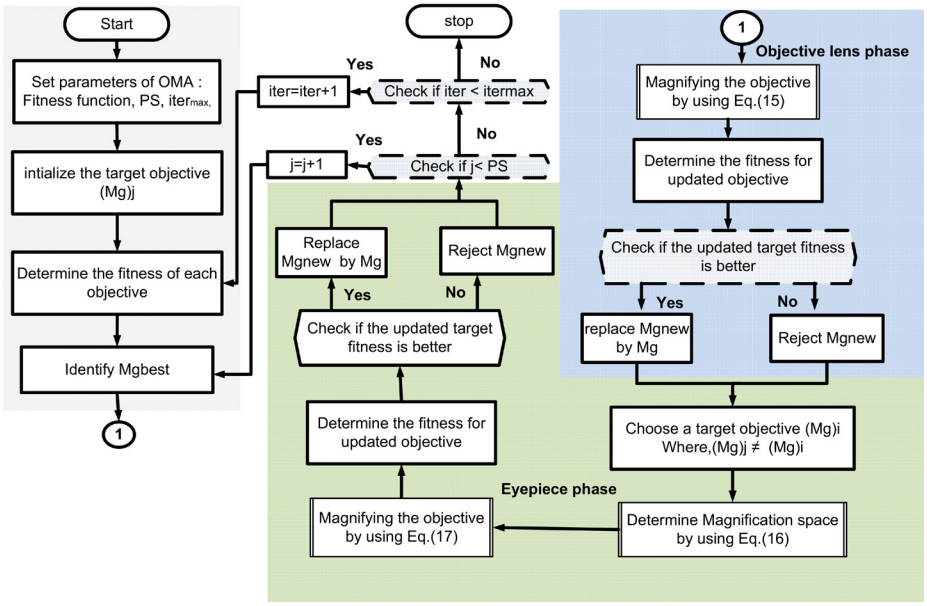

FIGURE 3. Flowchart of basic optical microscope algorithm (OMA).

data of the next time steps is not available for the optimizer. It has an input membership varying with the change of the PV or wind output power. Therefore, any change in environmental conditions will be considered, and this may lead to change a state of charging to a state of discharging. The uncertain conditions can be analyzed using different approaches, like Monte Carlo Simulation (MCS), which is a straightforward approach but needs time to compute and memory. Another approach, Point Estimate Method (PEM), is simpler and solves the stochastic problem faster with the ability to investigate the uncertain problem that includes load variation forecasting and wind speed [46], [47], [48], [49]. The fuzzy logic is modeled to calculate the penalty factor, which can handle the uncertain conditions such as wind speed and load variation. Fuzzy logic has been able to handle many forms of uncertainty within a single conceptual framework by combining predicate logic and probability theory. The time-varying inputs that suffer from uncertainty have been defined as uncertain sets to account for all possible conditions by converting them to a type-2 fuzzy set. The sets of inputs and output are:

- Real-time pricing: Low (L), Medium (M), and high (H).
- SOC: very low, low, medium, high, and very high.
- Pnet: Negative Big (NB), Negative Medium (NM), Negative Small (NS), Zero (ZE), Positive Small (PS), Positive Medium (PM), and Positive Big (PB).
- penF: very low, low, medium, high, and very high.

Human logic enhances the dynamic penalty factor, which saves operation costs and improves the storage system's performance. FL consists of 87 rules that can further explain and clarify their concept of operation as **If (Pnet is NB) and (Real-time pricing is H) and (SOC is medium) then (PenF is very-low)**. In this condition, a great gap exists between the generation and load, and the generation power can't cover the demand during high-price periods while the SOC is medium. It results in FL making the penalty factor very low, causing the maximum discharge of the battery to meet the load and reducing the number of purchasing units to minimize the cost. Another example for rules is **If (Pnet is PS) and (Real-time pricing is M) and (SOC is low) then (PenF is high)**. In this case, the real-time price is medium and the generation power is a little over the demand while the SOC is low. Therefore, the fuzzy logic decided to make the penalty factor high to prevent the battery from discharging and guide the algorithm to charge the battery for the next time steps. The medium price periods have no advantage in selling energy to the main grid or purchasing energy. During this period, the system charges the battery if there is enough energy and the SOC is not enough for the next steps. However, the demand is greater. The fuzzy logic decides on buying energy from the main grid or not depending on the SOC. Similarly, the remaining rules describe human logic and it is listed three more:

- If(Pnet is PB) and (Real-time pricing is H) and (SOC is medium) then (PenF is medium).
- If (Pnet is ZE) and (Real-time pricing is L) and (SOC is high) then (PenF is high).
- If (Pnet is PS) and (Real-time pricing is L) and (SOC is very-high) then (PenF is very-high).

C. CONVOLUTION NEURAL NETWORKS

It is a powerful tool for image processing and data analysis with different dimensionalities. CNN is used for various purposes such as classification and forecasting in different fields weather forecasting, medicine, classification of electrical faults, and islanding [50]. Feeding CNN with a huge dataset and different parameters builds a robust model. The convolution operator is the main mathematical representation

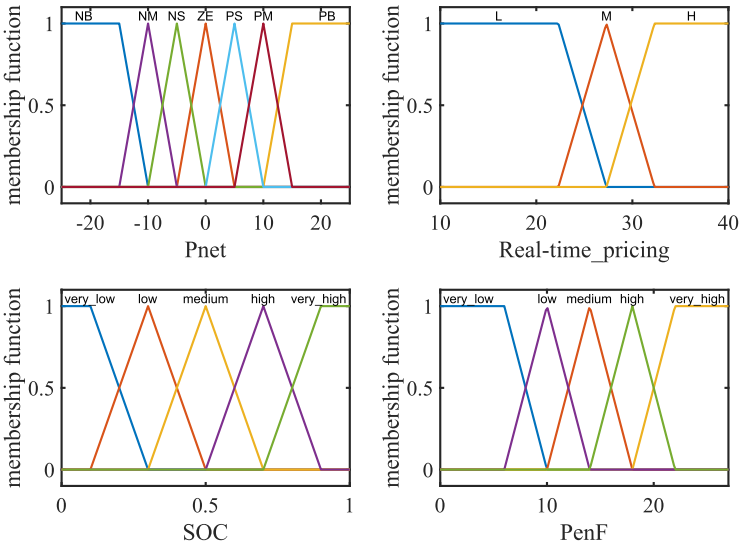

FIGURE 4. Memberships of fuzzy logic.

and is described as [51]:

$$output(i) = \sum_{i,j} input(i-j)weight(j) \tag{18}$$

where i is the vertical step of the filter, while the horizontal step is j. The convolution stage extracts the features. Initially, the kernel and filter are convolved with the input, and the result is added to a bias term. This process is repeated until the complete feature map is obtained. The convolution operation and the subsequent activation function can be expressed as [52]:

$$output_{ij}^{k} = Bt_k + \sum_{ij} km_k \times fm_{ij} \tag{19}$$

$$fun_{active} = activation(output^{k}) \tag{20}$$

where k introduces the k^{th} feature maps. The output is given by $output_{ij}^{k}$. The filter matrix and the kernel matrix are presented by fm_{ij} and km_k respectively. The fun_{active} is the activation function's output. Pooling Layers reduce the spatial dimensions of the feature maps while keeping the input data quality. This dimension-reduction process is useful because it prepares the model to learn the parameters using the back-propagation algorithm, and then the fully Connected Layers perform classification or regression based on the learned features. The output Layer Provides the final prediction. When CNN is trained on these signal images and learns to associate specific patterns in the signal, it will be able to classify new signal data by converting it into an image format and passing it through. The CNN architecture is shown in Fig.5 CNN detects the islanding of the microgrid or not by analyzing the waveforms of the fundamental phase value voltages and currents and the second-order harmonics phase value of voltages and currents and feeds the output to the scheme for making the optimal decision of operation in real-time operation [53]. The measured voltage and current signals at PCC between the grid and the microgrid are processed using the discrete Fourier transform (DFT). Under islanding conditions, this process increases the second harmonic component of both voltage and current [1]and leads to undervoltage similar to the Sandia Voltage Shift method [11]. The harmonic components generated during islanding are extracted from the simulated model and converted into a visual format, typically as images using a sampling frequency equal to 1 kHz. This can be achieved via mapping the signal data into pixel intensities and scaling the signal values, then reshaping to a matrix form. The pixel data can be tackled as an input image for a CNN. The convolution layer applies filters (kernels) to the input images to detect features, while the activation layers introduce nonlinearity to the network, enabling it to learn complex relationships in the data. A total 5300 samples were obtained from the simulation for islanding and non-islanding cases. These cases covered most of the conditions of power mismatch or the number of renewable generator units. It can be divided into 3400 non-islanding samples and 1900 islanding samples, where 70% of this dataset was used for training while the remaining 30% is used for testing. The false positive/negative rate is used to evaluate CNN's performance by defining the F1-measure, accuracy, sensitivity, and precision. The CNN's performance was determined by feeding these parameters into the confusion matrix. The percentage of relevant samples that have been retrieved out of all the relevant samples is known as sensitivity. Precision is the fraction of relevant samples among the retrieved samples. The parameters are calculated using the following equations [53].

$$\text{Accuracy} = \frac{TP + TN}{TP + FP + FN + TN} \tag{21}$$

$$Sensitivity = \frac{TP}{TP + FN} \tag{22}$$

$$\text{Precision} = \frac{TP}{TP + FP} \tag{23}$$

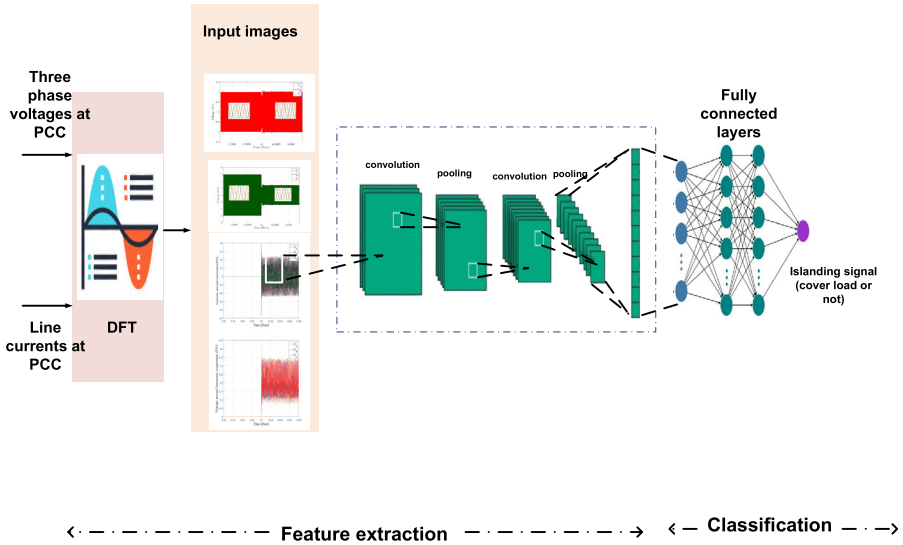

FIGURE 5. The proposed CNN.

$$\text{F1 measure} = \frac{2 \times (\text{Precision} \times \text{Sensitivity})}{(Precision + \text{Sensitivity})} \quad (24)$$

VI. NUMERICAL IMPLEMENTATION AND RESULTS

A dynamic optimal energy management scheme has been numerically implemented on a grid-connected microgrid model established on MATLAB. The optimal operation of the microgrid generating units as well as the storage system, has been accomplished under normal and islanding conditions. Through the dynamic approach of this scheme, fuzzy logic rules have been utilized in conjunction with the optimization technique to guide the algorithm according to the operating conditions at each time step. While CNN has detected the islanding condition and a signal has been sent to the optimizer upon its occurrence. Three different optimization algorithms have been applied to recommend the most suitable one for this complex scheme. Five scenarios have been investigated during both normal and islanding conditions. The optimal process achieves a minimum operating cost and ensures uninterrupted service to the load. The baseline approach is the most common method that has been used in power management based on an if-else statement for the minimum operating cost of the microgrid. In this technique, the charging process of the storage system is carried out when the generating power of the renewable units is over the load demand. After that, if there is remaining energy, it will be sold to the grid. The discharging process has been accomplished when the renewable generators couldn't support the load demand, and if the storage system couldn't support the load demand, the required load demand will be purchased from the main grid. This means that the storage system is controlled according to the availability of energy and the balance between generation and demand. Therefore, it doesn't have any target to make a profit by using the storage system, and the real-time price of electricity is not considered in the baseline approach. On the contrary, in the proposed dynamic approach, the real-time prices are evaluated continuously, and the storage system is controlled via FL to be a part of achieving profits and maximizing net savings. The proposed methodology was numerically implemented and validated on a simulated model within the main program, using real location data. A case study was conducted for a system located in California (Latitude 36°28'55.41" N, Longitude 120°15'05.55" W), consisting of a microgrid connected to the main grid. The wind speed, and irradiance data are shown in figure 6 where islanding occurred in time slots 10, 16,17,31,42,43,44, and 58. The accuracy, sensitivity, precision and F1 measure of the false positive/negative rate are equal to 0.9967, 0.9992, 0.9963, and 0.9977, respectively. The baseline approach has been presented through the following figures 7 that provide the power curves of each element and the amount of energy exchanged with the main grid. The baseline cost was calculated by equation 7 and equaled 6395.9 cents. Three optimization algorithms have been tested: Quadratic Interpolation Optimization(QIO), Hunger Games Optimizer(HGO), and OMA, and the results have been compared to select the most efficient one. The following formula determines the savings to compare the results based on the baseline technique [21]:

$$\text{percentage Saving}\% = \frac{C_{Baseline} - C_{optm}}{C_{Baseline}} \times 100\% \quad (25)$$

where C_{optm} provides the cost calculated from the algorithm's decisions. $C_{Baseline}$ presents the baseline's cost.

Three algorithms have been numerically implemented with the objective equation 8 as:

Algorithm 1 Structure of the Proposed Methodology

Inputs: irradiance, ambient temperature, load, and wind speed. Population size PS, the maximum number of iterations $iter_{max}$, and the islanding signal.
Outputs: The operation of the biomass generator, the amount of energy exchanged with the battery bank, buying/selling energy from the main grid, and the decision of operating the microgrid during islanding or not.
time slot=1;
while (time slot < time horizon) **do**
    Step 1: estimate the initial target.
    Step 2: FL provides the penalty factor and CNN monitoring islanding.
    Step 3: Calculate the fittness by equation 8 from the initial target.
    while (number of iteration < $iter_{max}$) **do**
        for (every potential target) **do**
The magnification space has been updated based on the OMA equations. (15 to 17).
        Step 4: Check islanding and the ability of the microgrid to cover the load.
        if no islanding detection **then**
            Step 5: Calculate the penalty factor and estimate the fitness of equation 8.
        else
            if the microgrid can cover the load **then**
                Step 6: continue feeding the demand.
            else
                Step 7:disconnect the microgrid.
    time slot=time slot+1;
Display: *The optimum solution for the battery bank, biomass generator, renewable generators, and grid .*

- OMA: It is obvious that the OMA optimization technique achieves the best solution for the microgrid where the operating cost is equal to -7909.66 cents and the saving ratio is 223.4 %. The power of the MG over a time horizon of the proposed scheme can be shown in figure 8 while the energy exchanging with the main grid and the cycles of the battery can be shown in Figure 9.
- Hunger Games Optimizer: it has an operating cost equal to -7895.224 cents with a saving percentage of 223.4 %. The following curves 10 and 11 show the power of each element and the power exchange with the main grid.
- QIO: in this case, the cost is −7297.29 cents and the saving 214.1 % to baseline. This algorithm gives the lowest benefit among the other algorithms. The output power of the MG components and the energy of the main grid can be provided in figures 12 and 13 respectively.

The summary of the results obtained above can be found in Table1. The positive sign means the operating cost is more than the revenue, while the negative sign indicates that the revenue from selling energy into the grid is greater than the operating cost. The convergence curves of HGO and OMA

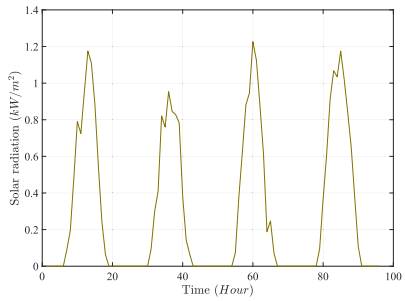

(a) irradiance.

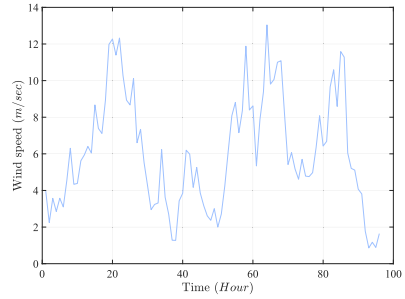

(b) Wind speed.

FIGURE 6. **The inputs of the proposed approach.**

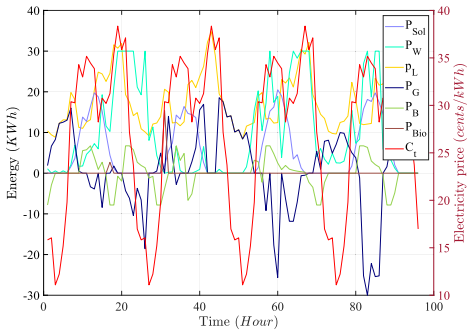

(a) power of the MG elements.

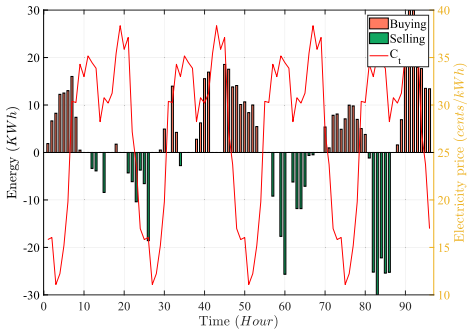

(b) the grid's energy.

FIGURE 7. **Baseline approach.**

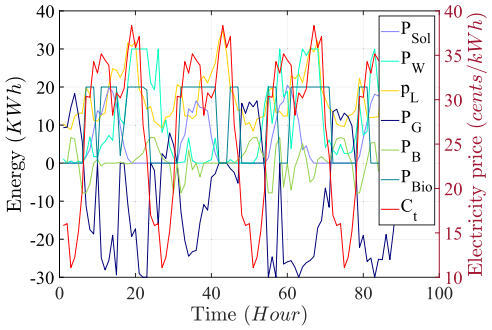

FIGURE 8. Power of the MG elements for OMA over the five scenarios.

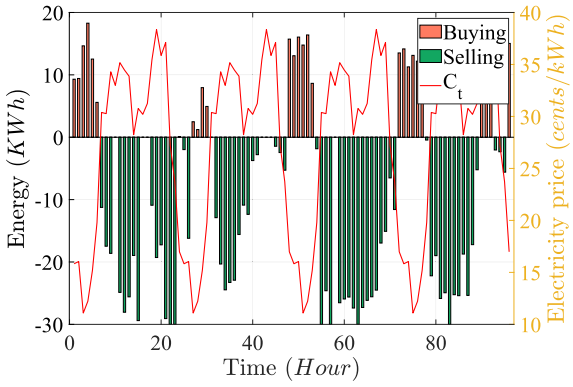

(a) the main grid's energy.

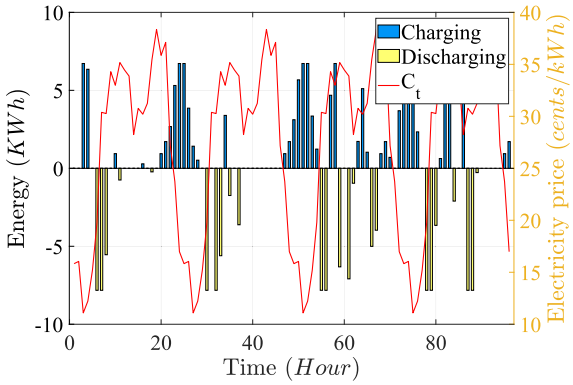

(b) battery cycles.

FIGURE 9. The proposed approach with OMA.

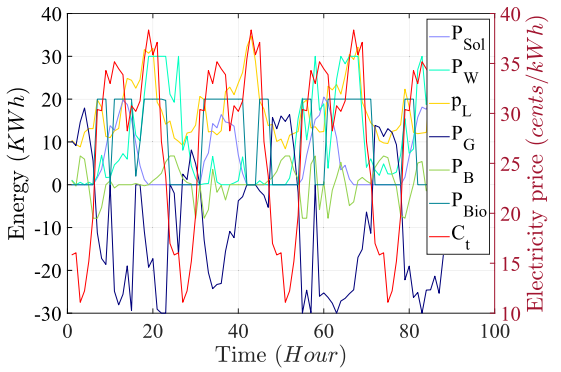

FIGURE 10. Power of the MG elements for HGO over the five scenarios.

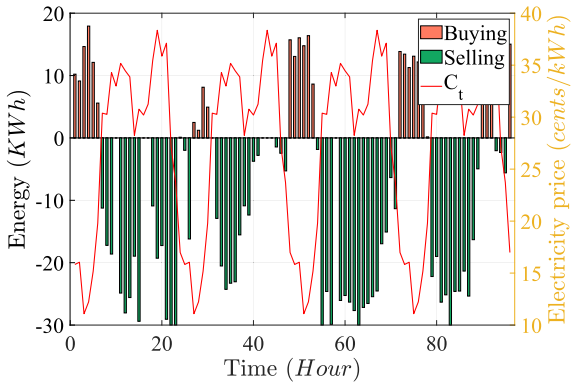

(a) the main grid's energy.

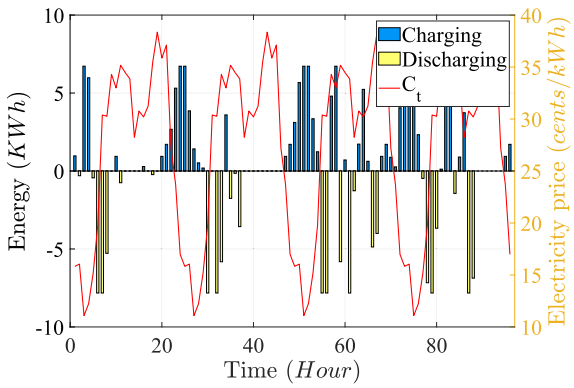

(b) battery cycles.

FIGURE 11. The proposed approach with HGO.

can be shown in Figure 14, which shows that OMA has a higher speed of convergence.

The results of an OMA optimizer paired with fuzzy logic rules to extract the optimal solution of the problem can be verified via five scenarios. The different actions of the optimizer can be clarified in each scenario.

A. THE FIRST SCENARIO

It presents the normal operation of the MG and provides the optimal solution for MG operation. The numerical implementation of OMA and the fuzzy strategy can achieve optimal operation according to the availability of power, real-time pricing, and SOC. The FL determines the penalty factor value at each time step to improve and enhance the capability of the energy management of the MG and make the proper decision for the battery as well as the biomass operation by applying the equation 8 dynamically. In time

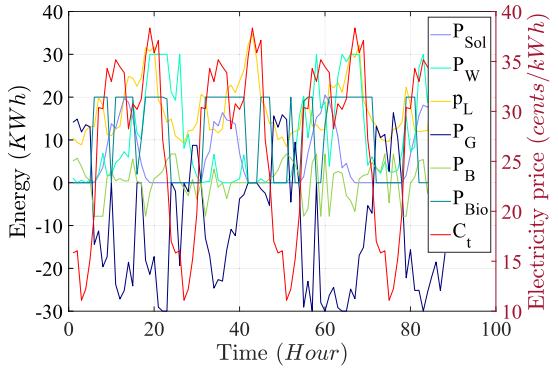

FIGURE 12. Power of the MG elements for QIO the five scenarios.

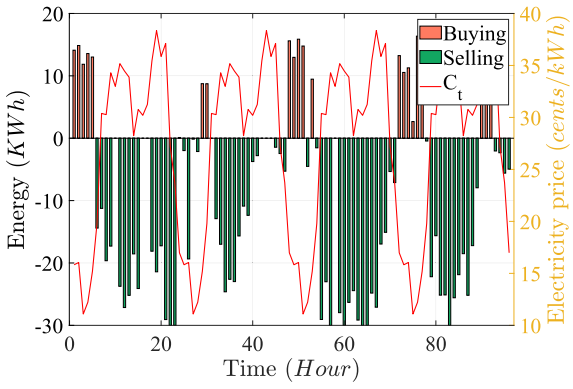

(a) the main grid's energy.

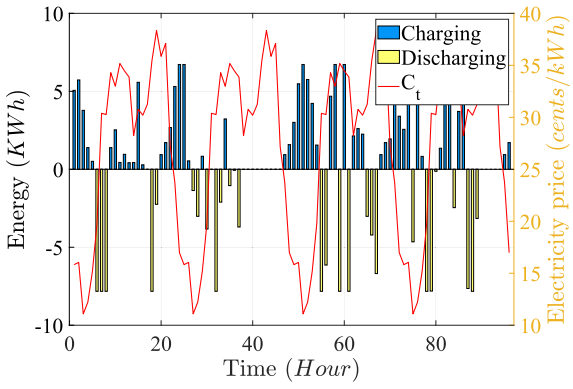

(b) battery cycles.

FIGURE 13. The proposed approach with QIO.

slot 8, the real-time pricing is 30.27 cents / kWh, and the demand exceeds the renewable generation energy. As a result, the command decision leads to the discharge of energy equal to 5.543 kWh. The biomass generator operates at maximum rated power to cover the load and sells the additional energy to the main grid to achieve a profit during the high pricing period. The time-of-use price reaches 37.12 cents/ kWh

TABLE 1. Summarized results for different algorithms.

Algorithm	Cost(cents)	Net saving (%)	conv-time(sec)
Baseline	6395.9	0	-
OMA	-7909.66	223.7	14.076
QIO	-7297.29	214.1	232.6057
HGO	-7895.224	223.4	67.2596

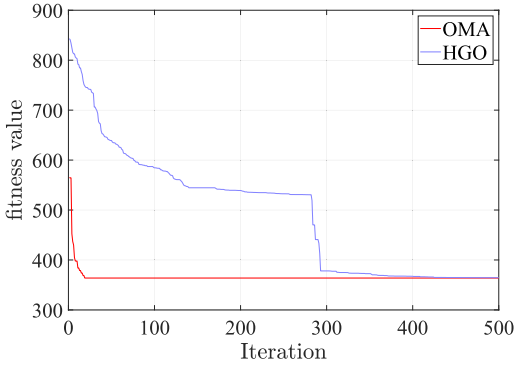

FIGURE 14. Convergence curves of HGO and OMA.

in time slot 21. However, the generated renewable energy exceeds the demand by 10.7 kWh. The decision is the biomass generator output and the remaining units sold to the grid. In contrast, the remaining energy of (1.7 KWh) is charged to the battery because of the low priority to charge as the priority is to sell energy during very high price periods. The methodology of the scheme at time slot 51 which has very low real-time pricing equal to 11.088 cents/kWh is different according to the operating conditions. The load is still higher than the renewable generation but the battery bank is operating in charging mode with a charging energy of 6.721 KWh to increase the SOC during low-cost periods and use this energy during high-cost periods or islanding. The biomass generator is shut down and the energy difference is bought from the grid. Finally, the price is almost medium and equal to 28.24 Cents/kWh while the generated energy exceeds the load in time slot 86. Therefore, the FL finds no advantage in buying or selling energy so the excess energy is charged to the battery bank without requiring the operation of the biomass generator. Figure 15 presents the microgrid simulation model. CNN detects the islanding and sends a signal to the main algorithm. The microgrid performance analysis will be tested during the next scenarios to compare the difference in islanding detection during different loading conditions.

B. THE SECOND SCENARIO

The second scenario occurs when the microgrid operates at islanding conditions while the power generation from the MG exceeds the load that buys into the main grid. At time slot 10, the power generated is 14.86 KW while the load is

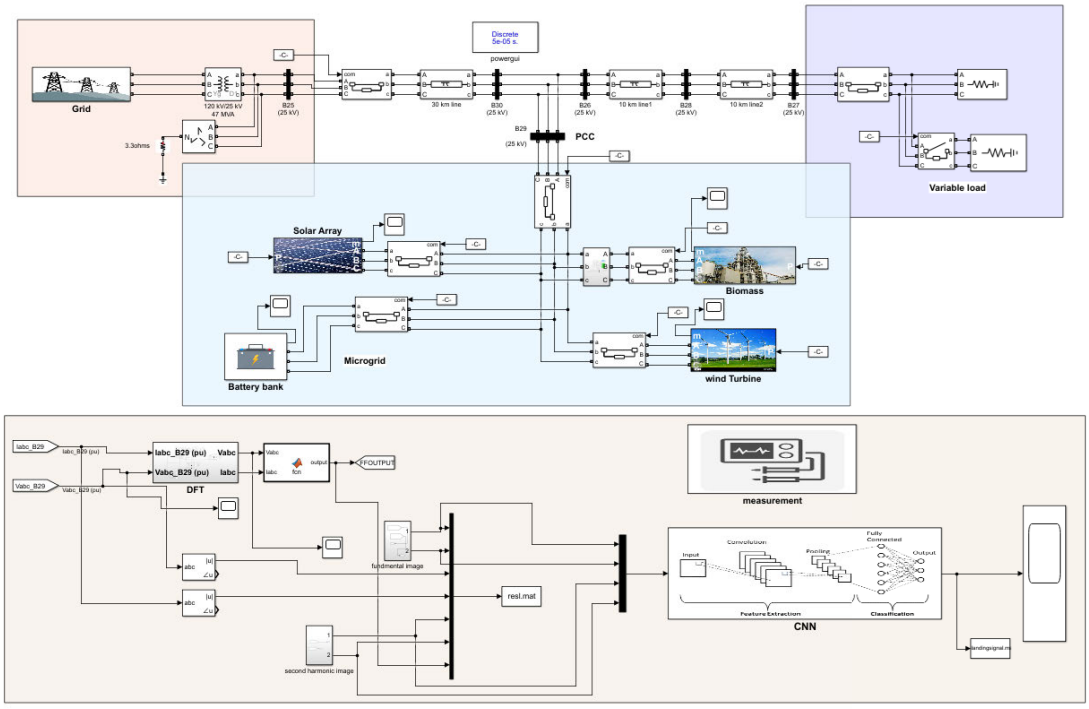

FIGURE 15. Simulation model of the microgrid.

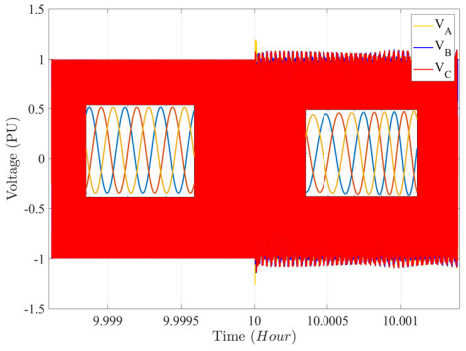

(a) Three phase fundamental voltage waveforms.

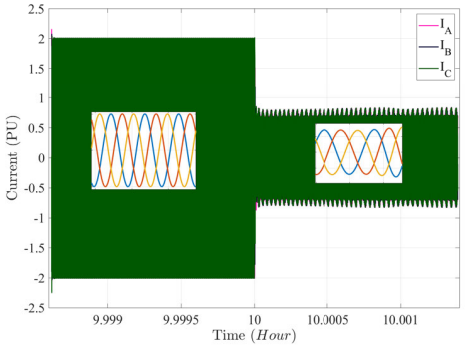

(b) Three lines fundamental current waveforms.

FIGURE 16. Waveforms in slot time 10.

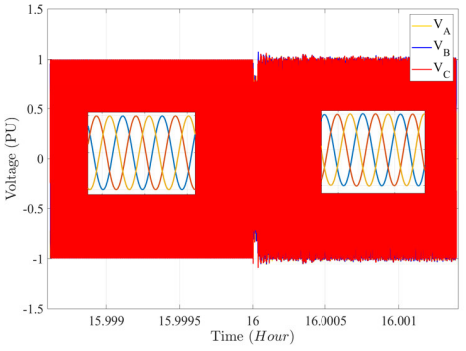

(a) Three phase fundamental voltage waveforms.

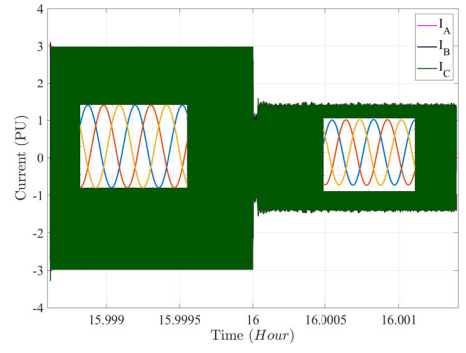

(b) Three lines fundamental current waveforms.

FIGURE 17. Waveforms in slot time 16.

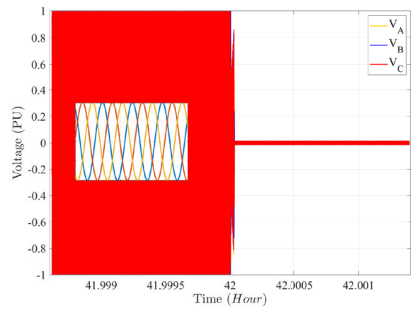

(a) Three phase fundamental voltage waveforms.

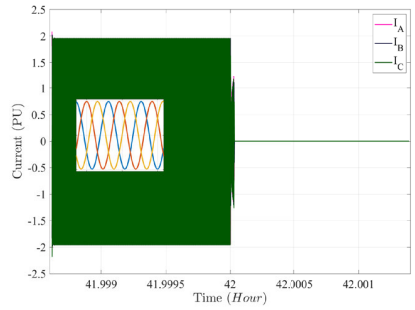

(b) Three lines fundamental current waveforms.

FIGURE 18. Waveforms in slot time 42.

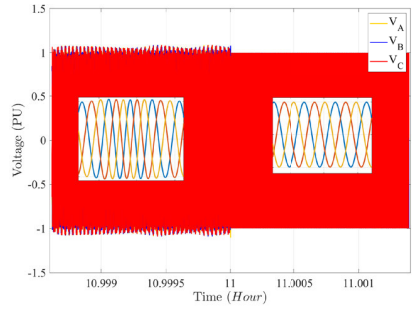

(a) Three phase fundamental voltage waveforms.

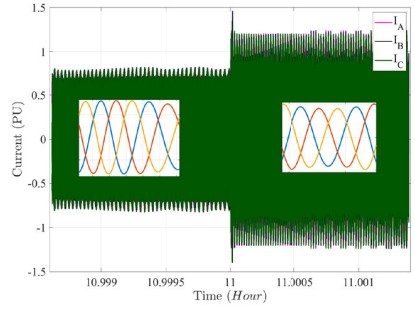

(b) Three lines fundamental current waveforms.

FIGURE 19. Waveforms in slot time 11.

11.01 KW. The CNN detects islanding occurrence at this time slot from the input waveforms of voltages and currents of the fundamentals and the dominant harmonics in the signals caused by islanding that are shown in Figure 16. However, the MG can cover the load so the fundamental voltage waveforms don't drop. The current was reduced as a result of the grid disconnection, and MG stopped buying energy. The decision is to continue to supply the load and the excess energy is used to charge the battery while the biomass is shut off. Therefore, the MG can operate during the islanding without any risk of damage to its elements.

C. THE THIRD SCENARIO

In scenario three, the islanding occurs and the generation power and the battery bank, cannot cover the load at time slot 16, The voltages dropped when the islanding was detected, then the biomass was connected and the voltage was restored to its normal magnitude as shown in figure 17 where the biomass generator compensates for the difference between the load and the generation during islanding, which leads in turn to the safe operation of the MG and ensures its continuity of service to the load.

D. THE FOURTH SCENARIO

The load exceeded the generated power and the stored power, and even upon the operation of biomass at its rated condition, the load can't be fulfilled. This case has been investigated at a time slot 42. As a result, the decision is to disconnect the MG to save its components from damage. The figure 18 shows the drop of the voltage waveforms under a certain value with increasing the second-order harmonics component. This case forced the scheme to disconnect the MG and wait until the main grid was back in operation.

E. THE FIFTH SCENARIO

In this scenario, when the islanding signal has ended at time slot 11, the harmonics superimposed on the fundamental voltage have vanished and the fundamental voltages are restored. while the harmonics on the current are damped with time progress, and the proposed scheme can detect the clearance of islanding conditions and restore normal operation automatically. The voltage and current signals are shown in Figure 19.

VII. CONCLUSION

In the grid-connected microgrid, a smart novel methodology has been proposed to provide an economical and dynamic solution to the islanding problem proposed to detect islanding and to maintain the continuity of service to the load at a time rather than disconnecting the microgrid and interrupting the service to the load. A neuro-fuzzy-optical microscope optimizer scheme has been introduced to integrate islanding detection and online optimal power management. To validate the proposed scheme, many cases have been investigated and tested with the aid of various optimization techniques to prove the outstanding performance of the proposed scheme in detecting and solving the islanding problem, in addition to preventing interruption of service to the load when the main

grid has been disconnected without causing any damage to the components of the microgrid.

REFERENCES

[1] A. G. Abd-Elkader, D. F. Allam, and E. Tageldin, "Islanding detection method for DFIG wind turbines using artificial neural networks," *Int. J. Electr. Power Energy Syst.*, vol. 62, pp. 335–343, Nov. 2014.

[2] W. Cai, B. Liu, S. Duan, and C. Zou, "An islanding detection method based on dual-frequency harmonic current injection under grid impedance unbalanced condition," *IEEE Trans. Ind. Informat.*, vol. 9, no. 2, pp. 1178–1187, May 2013.

[3] M. W. Altaf, M. T. Arif, S. Saha, S. N. Islam, M. E. Haque, and A. M. T. Oo, "Effective ROCOF-based islanding detection technique for different types of microgrid," *IEEE Trans. Ind. Appl.*, vol. 58, no. 2, pp. 1809–1821, Mar. 2022.

[4] C. R. Reddy, J. H. Choi, and B. Pangedaiah, "Absolute positive sequence voltage difference based passive islanding detection in micro grids," *IEEE Trans. Ind. Appl.*, vol. 60, no. 3, pp. 4633–4641, May 2024.

[5] R. Nale, M. Biswal, N. Kishor, J. Merino, A. Perez-Basante, and J. E. Rodriguez-Seco, "Real-time analysis of islanding detection scheme developed for AC microgrid system," *Electric Power Syst. Res.*, vol. 226, Jan. 2024, Art. no. 109926.

[6] M. S. Kulkarni, S. Mishra, S. K. Sudabattula, N. K. Sharma, D. B. Basha, M. Bajaj, and M. B. Tuka, "Enhancing grid resiliency in distributed energy systems through a comprehensive review and comparative analysis of islanding detection methods," *Sci. Rep.*, vol. 14, no. 1, p. 12124, May 2024.

[7] N. Shafique, S. Raza, S. Bibi, M. Farhan, and M. Riaz, "A simplified passive islanding detection technique based on susceptible power indice with zero NDZ," *Ain Shams Eng. J.*, vol. 13, no. 4, Jun. 2022, Art. no. 101637.

[8] R. Reddy, G. R. Reddy, B. S. Goud, N. Rajeswaran, and N. Kumar, "Passive islanding detection methods for integrated distributed generation system," *J. Power Technol.*, vol. 101, no. 3, pp. 1–8, 2021.

[9] B. Eristi, V. Yamacli, and H. Eristi, "A novel microgrid islanding classification algorithm based on combining hybrid feature extraction approach with deep ResNet model," *Electr. Eng.*, vol. 106, no. 1, pp. 145–164, Feb. 2024.

[10] O. A. Allan and W. G. Morsi, "A new passive islanding detection approach using wavelets and deep learning for grid-connected photovoltaic systems," *Electric Power Syst. Res.*, vol. 199, Oct. 2021, Art. no. 107437.

[11] P. Puranik, B. Prabhu, A. Saligram, and K. Suryanarayana, "Islanding detection of grid-connected photovoltaic systems using active disturbance-based techniques," in *Advances in Renewable Energy and Electric Vehicles: Select Proceedings of AREEV 2020*. Cham, Switzerland: Springer, 2022, pp. 261–275.

[12] M. A. Khan, A. Haque, V. S. B. Kurukuru, and M. Saad, "Islanding detection techniques for grid-connected photovoltaic systems–A review," *Renew. Sustain. Energy Rev.*, vol. 154, Feb. 2022, Art. no. 111854.

[13] P. A. Pegoraro, K. Brady, P. Castello, C. Muscas, and A. von Meier, "Compensation of systematic measurement errors in a PMU-based monitoring system for electric distribution grids," *IEEE Trans. Instrum. Meas.*, vol. 68, no. 10, pp. 3871–3882, Oct. 2019.

[14] N. Gupta, R. Dogra, R. Garg, and P. Kumar, "Review of islanding detection schemes for utility interactive solar photovoltaic systems," *Int. J. Green Energy*, vol. 19, no. 3, pp. 242–253, Feb. 2022.

[15] A. Hussain, C.-H. Kim, and A. Mehdi, "A comprehensive review of intelligent islanding schemes and feature selection techniques for distributed generation system," *IEEE Access*, vol. 9, pp. 146603–146624, 2021.

[16] M. M. Islam, T. Yu, G. Giannoccaro, Y. Mi, M. La Scala, M. R. Nasab, and J. Wang, "Improving reliability and stability of the power systems: A comprehensive review on the role of energy storage systems to enhance flexibility," *IEEE Access*, vol. 12, pp. 152738–152765, 2024.

[17] P. García, J. P. Torreglosa, L. M. Fernández, and F. Jurado, "Optimal energy management system for stand-alone wind turbine/photovoltaic/hydrogen/battery hybrid system with supervisory control based on fuzzy logic," *Int. J. Hydrogen Energy*, vol. 38, no. 33, pp. 14146–14158, Nov. 2013.

[18] M. Tekin, D. Hissel, M.-C. Pera, and J. M. Kauffmann, "Energy-management strategy for embedded fuel-cell systems using fuzzy logic," *IEEE Trans. Ind. Electron.*, vol. 54, no. 1, pp. 595–603, Feb. 2007.

[19] G. K. Venayagamoorthy, R. K. Sharma, P. K. Gautam, and A. Ahmadi, "Dynamic energy management system for a smart microgrid," *IEEE Trans. Neural Netw. Learn. Syst.*, vol. 27, no. 8, pp. 1643–1656, Aug. 2016.

[20] T. Adefarati and R. C. Bansal, "Reliability, economic and environmental analysis of a microgrid system in the presence of renewable energy resources," *Appl. Energy*, vol. 236, pp. 1089–1114, Feb. 2019.

[21] Y. O. Shaker, D. Yousri, A. Osama, A. Al-Gindy, E. Tag-Eldin, and D. Allam, "Optim rging decision of energy storage community in grid-connected microgrid using multi-objective hunger game search optimizer," *IEEE Access*, vol. 9, pp. 120774–120794, 2021.

[22] M. R. Nasab, R. Cometa, P. Ghalebani, S. Bruno, and M. L. Scala, "Distributed adaptive droop control method for flexibility enhancement of islanded DC microgrids including electric springs," in *Proc. Energy Convers. Congr. Expo Eur.*, Mar. 2024, pp. 1–6.

[23] N. Gudi, L. Wang, and V. Devabhaktuni, "A demand side management based simulation platform incorporating heuristic optimization for management of household appliances," *Int. J. Electr. Power Energy Syst.*, vol. 43, no. 1, pp. 185–193, Dec. 2012.

[24] D. Fuselli, F. De Angelis, M. Boaro, S. Squartini, Q. Wei, D. Liu, and F. Piazza, "Action dependent heuristic dynamic programming for home energy resource scheduling," *Int. J. Electr. Power Energy Syst.*, vol. 48, pp. 148–160, Jun. 2013.

[25] M. A. Hossain, H. R. Pota, S. Squartini, and A. F. Abdou, "Modified PSO algorithm for real-time energy management in grid-connected microgrids," *Renew. Energy*, vol. 136, pp. 746–757, Jun. 2019.

[26] A. A. Z. Diab, H. M. Sultan, and O. N. Kuznetsov, "Optimal sizing of hybrid solar/wind/hydroelectric pumped storage energy system in Egypt based on different meta-heuristic techniques," *Environ. Sci. Pollut. Res.*, vol. 27, no. 26, pp. 32318–32340, Sep. 2020.

[27] M. Jahannoosh, S. A. Nowdeh, A. Naderipour, H. Kamyab, I. F. Davoudkhani, and J. J. Klemeš, "New hybrid meta-heuristic algorithm for reliable and cost-effective designing of photovoltaic/wind/fuel cell energy system considering load interruption probability," *J. Cleaner Prod.*, vol. 278, Jan. 2021, Art. no. 123406.

[28] M. A. Hossain, H. R. Pota, S. Squartini, F. Zaman, and J. M. Guerrero, "Energy scheduling of community microgrid with battery cost using particle swarm optimisation," *Appl. Energy*, vol. 254, Nov. 2019, Art. no. 113723.

[29] J. F. Manwell and J. G. McGowan, "Lead acid battery storage model for hybrid energy systems," *Sol. Energy*, vol. 50, no. 5, pp. 399–405, May 1993.

[30] M. B. Eteiba, S. Barakat, M. M. Samy, and W. I. Wahba, "Optimization of an off-grid PV/biomass hybrid system with different battery technologies," *Sustain. Cities Soc.*, vol. 40, pp. 713–727, Jul. 2018.

[31] C. Ghenai and I. Janajreh, "Design of solar-biomass hybrid microgrid system in sharjah," *Energy Proc.*, vol. 103, pp. 357–362, Dec. 2016.

[32] M. M. Samy, H. H. Sarhan, S. Barakat, and S. A. Al-Ghamdi, "A hybrid PV-biomass generation based micro-grid for the irrigation system of a major land reclamation project in kingdom of Saudi Arabia (KSA)—Case study of albaha area," in *Proc. IEEE Int. Conf. Environ. Electr. Eng. IEEE Ind. Commercial Power Syst. Eur. (EEEIC / I&CPS Europe)*, Jun. 2018, pp. 1–8.

[33] G. Shi, Q. Wei, and D. Liu, "An adaptive dynamic programming based method for optimization of electricity consumption in office buildings," in *Proc. Int. Joint Conf. Neural Netw. (IJCNN)*, Jul. 2016, pp. 4551–4556.

[34] M. Boaro, D. Fuselli, F. D. Angelis, D. Liu, Q. Wei, and F. Piazza, "Adaptive dynamic programming algorithm for renewable energy scheduling and battery management," *Cognit. Comput.*, vol. 5, no. 2, pp. 264–277, Jun. 2013.

[35] G. Shi, Q. Wei, and D. Liu, "Optimization of electricity consumption in office buildings based on adaptive dynamic programming," *Soft Comput.*, vol. 21, no. 21, pp. 6369–6379, Nov. 2017.

[36] M. A. Hossain, R. K. Chakrabortty, M. J. Ryan, and H. R. Pota, "Energy management of community energy storage in grid-connected microgrid under uncertain real-time prices," *Sustain. Cities Soc.*, vol. 66, Mar. 2021, Art. no. 102658.

[37] H. A. Gabbar and A. A. Abdelsalam, "Microgrid energy management in grid-connected and islanding modes based on SVC," *Energy Convers. Manage.*, vol. 86, pp. 964–972, Oct. 2014.

[38] *Environment Compatibility Levels for Low-frequency Conducted Disturbances and Signaling in Public Low-voltage Power Supply Systems*, Standard IEC 61000-2-2, 2009.

[39] L. Guo and W. Gu, "PMSOMA: Optical microscope algorithm based on piecewise linear chaotic mapping and sparse adaptive exploration," *Sci. Rep.*, vol. 14, no. 1, p. 20849, Sep. 2024.
[40] D.-H. Tran, K.-N. Tran, and N. H. Nguyen, "A novel hybrid multiple objective optical microscope algorithm for fuzzy time, cost, and quality tradeoff in project management," *Int. J. Construction Manage.*, vol. 25, no. 10, pp. 1–13, Jul. 2025.
[41] S. Hou, H. Yin, B. Pla, J. Gao, and H. Chen, "Real-time energy management strategy of a fuel cell electric vehicle with global optimal learning," *IEEE Trans. Transp. Electrific.*, vol. 9, no. 4, pp. 5085–5097, Dec. 2023.
[42] R. Gugulothu, B. Nagu, and D. Pullaguram, "Energy management strategy for standalone DC microgrid system with photovoltaic/fuel cell/battery storage," *J. Energy Storage*, vol. 57, Dec. 2023, Art. no. 106274.
[43] J. M. Mendel, *Explainable Uncertain Rule-Based Fuzzy Systems*. Cham, Switzerland: Springer, 2024.
[44] A. K. Varshney and V. Torra, "Literature review of the recent trends and applications in various fuzzy rule-based systems," *Int. J. Fuzzy Syst.*, vol. 25, no. 6, pp. 2163–2186, Sep. 2023.
[45] O. Castillo, J. R. Castro, and P. Melin, "Forecasting the COVID-19 with interval Type-3 fuzzy logic and the fractal dimension," *Int. J. Fuzzy Syst.*, vol. 25, no. 1, pp. 182–197, Feb. 2023.
[46] A. R. Abbasi and A. R. Seifi, "Simultaneous integrated stochastic electrical and thermal energy expansion planning," *IET Gener., Transmiss. Distribution*, vol. 8, no. 6, pp. 1017–1027, Jun. 2014.
[47] A.-R. Abbasi, R. Khoramini, B. Dehghan, M. Abbasi, and E. Karimi, "A new intelligent method for optimal allocation of D-STATCOM with uncertainty," *J. Intell. Fuzzy Syst.*, vol. 29, no. 5, pp. 1881–1888, Jul. 2015.
[48] A. R. Abbasi and A. R. Seifi, "Energy expansion planning by considering electrical and thermal expansion simultaneously," *Energy Convers. Manage.*, vol. 83, pp. 9–18, Jul. 2014.
[49] A. Kavousi-Fard, A. Abbasi, and A. Baziar, "A novel adaptive modified harmony search algorithm to solve multi-objective environmental/economic dispatch," *J. Intell. Fuzzy Syst.*, vol. 26, no. 6, pp. 2817–2823, Jun. 2014.
[50] Z. Li, F. Liu, W. Yang, S. Peng, and J. Zhou, "A survey of convolutional neural networks: Analysis, applications, and prospects," *IEEE Trans. Neural Netw. Learn. Syst.*, vol. 33, no. 12, pp. 6999–7019, Dec. 2022.
[51] J. Wu, "Introduction to convolutional neural networks," *Nat. Key Lab Novel Softw. Technology. Nanjing University. China*, vol. 5, no. 23, p. 495, 2020.
[52] B. Farsi, M. Amayri, N. Bouguila, and U. Eicker, "On short-term load forecasting using machine learning techniques and a novel parallel deep LSTM-CNN approach," *IEEE Access*, vol. 9, pp. 31191–31212, 2021.
[53] A. K. Ozcanli and M. Baysal, "Islanding detection in microgrid using deep learning based on 1D CNN and CNN-LSTM networks," *Sustain. Energy, Grids Netw.*, vol. 32, Dec. 2022, Art. no. 100839.

AHMED OSAMA was born in Faiyum, Egypt, in 1989. He received the Bachelor of Electrical Engineering and Machines degree and the M.Tech. degree from the Faculty of Engineering, Fayoum University, Faiyum, in 2011 and 2020, respectively, and the master's degree in high-voltage engineering with a focus on the mitigation of magnetic fields in 2020. He has ranked first in his graduation batch and his project is about automation control. Since January 2012, he has been an assistant at the Faculty of Engineering, Electrical Department, Fayoum University. He is a Research Team Member on smart grids and clean energy.

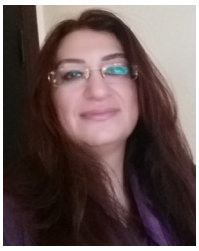

DALIA ALLAM received the B.Sc., M.Sc., and Ph.D. degrees in electrical power engineering from Cairo University, Egypt. She was certified as a Siemens Trainer in several automation subjects. She was the Ex-Manager of the Automatic Control Unit, Fayoum University, Egypt, where she is currently an Associate Professor with the Electrical Engineering Department. She has many publications in highly refereed international journals. Her research interests include applications of AI and SI in electrical power engineering, renewable energy, power quality, smart relays and digital protection systems, and automation and process control. She is also a reviewer for many international journals.

AHMED F. ZOBAA (Senior Member, IEEE) received the B.Sc. (Hons.), M.Sc., and Ph.D. degrees in electrical power and machines from Cairo University, Egypt, in 1992, 1997, and 2002, respectively, and the Doctor of Science degree from the Brunel University of London, U.K., in 2017. He received his Postgraduate Certificate in academic practice from the University of Exeter, U.K., in 2010. He was an Instructor from 1992 to 1997, a Teaching Assistant from 1997 to 2002, and an Assistant Professor from 2002 to 2007 at Cairo University, Egypt. From 2007 to 2010, he was a Senior Lecturer of renewable energy with the University of Exeter. From 2010 to 2019, he was a Senior Lecturer of power systems with the Brunel University of London, where he is currently a Reader of electrical and power engineering and a member with the Brunel Interdisciplinary Power Systems Research Centre. His research interests include power quality, (marine) renewable energy, smart grids, energy efficiency, and lighting applications. He is a registered Chartered Engineer, a Chartered Energy Engineer, an European Engineer, and an International Professional Engineer. He is also a Registered Member of the Engineering Council, U.K., Egypt Syndicate of Engineers, and Egyptian Society of Engineers. He is a Principal Fellow of the Higher Education Academy, U.K., a fellow of the Institution of Engineering and Technology, Energy Institute, U.K., the Chartered Institution of Building Services Engineers, U.K., the Institution of Mechanical Engineers, U.K., the Royal Society of Arts, U.K., and African Academy of Sciences. He is the Executive Editor-in-Chief of *Smart Grids and Sustainable Energy*. He is also an editorial board member, an editor, an associate editor, and an editorial advisory board member for many international journals.

MAGDY B. ETEIBA was born in Cairo, Egypt. He received the B.Sc. and M.Sc. degrees in electrical power from Ain Shams University, Cairo, Egypt, in 1970 and 1975, respectively, and the M.Eng. and Ph.D. degrees in electrical power from McGill University, Montreal, Quebec, Canada, in 1977 and 1982, respectively. He is currently an Emirates Professor with the Department of Electrical Engineering, Fayoum University, Faiyum, Egypt. He has published many papers and articles in international journals and conferences. His research interests include insulation and thermal characteristics of high-voltage equipment, transmission lines and cables, and development of renewable energy systems. He is a member of the National Committee for Higher Education Enhancement in Egypt.